



**Efficient modeling of organic adsorbates on oxygen-intercalated graphene on Ir(111)**Jari Järvi <sup>1,\*</sup>, Milica Todorović <sup>2</sup> and Patrick Rinke <sup>1</sup><sup>1</sup>*Department of Applied Physics, Aalto University, P.O. Box 11100, FI-00076 AALTO, Finland*<sup>2</sup>*Department of Mechanical and Materials Engineering, University of Turku, FI-20014 Turku, Finland*

(Received 20 December 2021; revised 13 April 2022; accepted 18 April 2022; published 9 May 2022)

Organic charge transfer complexes (CTCs) can be grown as thin films on intercalated graphene (Gr). Deciphering their precise film morphologies requires global *ab initio* structure search, where configurational sampling is computationally intractable unless we reconsider the model for the complex substrate. In this study, we employ charged freestanding Gr to approximate an intercalated Gr/O/Ir(111) substrate, without altering the adsorption properties of deposited molecules. We compare different methods of charging Gr and select the most appropriate substitute model for Gr/O/Ir(111) that maintains the adsorption properties of fluorinated tetracyanoquinodimethane (F<sub>4</sub>TCNQ) and tetrathiafulvalene (TTF), prototypical electron acceptor/donor molecules in CTCs. Next, we apply our model in the Bayesian optimization structure search method and density-functional theory to identify the stable structures of F<sub>4</sub>TCNQ and TTF on supported Gr. We find that both molecules physisorb to Gr in various configurations. The narrow range of adsorption energies indicates that the molecules may diffuse easily on the surface and molecule-molecule interactions likely have a central role in film formation. Our study shows that complex intercalated substrates may be approximated with charged freestanding Gr, which can facilitate exhaustive structure search of CTCs.

DOI: [10.1103/PhysRevB.105.195304](https://doi.org/10.1103/PhysRevB.105.195304)**I. INTRODUCTION**

Organic charge transfer complexes (CTCs), formed by electron acceptor and donor molecules, exhibit fascinating electronic properties, such as superconductivity [1] and charge density waves [2]. Their study has expanded from bulk crystals to organic thin films, which are typically grown on metal substrates [3,4]. However, hybridization of the molecular electronic states with the metal can interfere with their electronic properties. CTCs have therefore been grown on electronically decoupled graphene (Gr) [5], which can be obtained by intercalating a third species between Gr and metal as exemplified by atomic O and Ir(111) [6–11].

Fluorinated tetracyanoquinodimethane (F<sub>4</sub>TCNQ) and tetrathiafulvalene (TTF) (electron acceptor and donor, respectively) are prototypical organic molecules in CTCs [12–15]. On Gr/O/Ir(111) they self-assemble in different structural phases, which have been observed in microscopy images [15]. Precise knowledge of film morphologies can help in optimizing the properties of CTCs, and this can be acquired via global structure search using simulations. Detecting the structures requires thorough exploration of the large phase space of different molecular configurations. To accurately describe dispersive bonding between the molecules and the surface,

adsorption energies must be calculated with *ab initio* methods, such as density functional theory (DFT) [16,17]. This makes extensive sampling of different configurations very costly.

Recently, new machine learning methods have facilitated global *ab initio* structure search by reducing the amount of required energy calculations. For example, Bayesian inference [18] has been applied with DFT to resolve the structure of single-molecule adsorbates [19–23] and molecule pairs [24] on metals. Modeling configurations of multiple molecules requires a sizable surface area, and this combined with the complex intercalated substrate results in computationally expensive models. The substrate structure must therefore be approximated for efficient energy sampling, which can then be carried out with machine learning tools such as Bayesian Optimization Structure Search (BOSS) [22,23,25–27]. BOSS builds a surrogate model of the adsorption energy surface (AES) and utilizes uncertainty of the model for efficient exploration of the phase space.

Our objective is to build an approximate model of Gr/O/Ir(111) using isolated Gr. We introduce charge in freestanding Gr to mimic the doping of the Gr layer in intercalated Gr/O/Ir(111). We evaluate the accuracy of different models of charged Gr by checking how closely the approximated model reproduces the results of the full substrate. The approximated substrate can then be used in further adsorption studies. Here, we employ the approximate model to identify the stable adsorbate structures of F<sub>4</sub>TCNQ and TTF using the BOSS method. We analyze the electronic structure of the found configurations to study their charge transfer properties and extent of electronic coupling to the substrate. We focus on low-energy configurations, which are the best candidate

\*jari.jarvi@aalto.fi

structures to be used as building blocks in studying the formation of CTC monolayers.

In Sec. II, we first introduce the computational methods and models, and the adsorbate structure search with BOSS. In Sec. III A 1, we study the extent of electronic decoupling of Gr as a function of intercalated O coverage. Different approximate models of Gr/O/Ir(111) are compared in Sec. III A 2 for adsorbed F<sub>4</sub>TCNQ and TTF molecules. In Sec. III B 1, we identify stable structures of the molecules on the supported Gr model and study their electronic structure. We compare our structures to previous studies in Sec. III B 2, discuss our findings in Sec. IV, and conclude our study in Sec. V.

## II. METHODS

### A. Density-functional theory calculations

We use DFT [16,17] for all energy calculations and atomic structure relaxations. We employ the all-electron, numeric atom-centered orbital code FHI-AIMS [31–33] with the Perdew-Burke-Ernzerhof (PBE) [34] exchange-correlation functional. To model dispersive interactions for the complex organic-inorganic Gr/O/Ir(111) substrate and molecular adsorbates, we default to the standard Tkatchenko-Scheffler method [35] of applying van der Waals (vdW) corrections to the PBE functional.

We have used *light* real-space grid settings with tier-1 basis sets and a  $\Gamma$ -centered  $2 \times 2 \times 1$   $k$ -point mesh for our Gr/O/Ir(111) supercell models and the adsorption of F<sub>4</sub>TCNQ and TTF in global minimum configurations (Sec. III A). The local minima structures (Sec. III B) are recomputed with *tight* grids using tier-2 basis sets for more precise energetics. The projected density of states (pDOS) calculations employ a  $8 \times 8 \times 1$   $k$ -point mesh for Gr and  $4 \times 4 \times 1$  mesh for the adsorbed molecules. In the self-consistency cycle, the total energy is converged below  $10^{-6}$  eV and the structures are relaxed below a maximum force component of  $10^{-2}$  eV/Å. We employ Gaussian broadening of 0.1 eV for the electronic states and relativistic corrections with the zero-order regular approximation [36], and we use a dipole correction in the surface slab calculations [37]. Spin polarization is expected to have a negligible effect on the studied structures [38] so the calculations are performed spin unpolarized.

The Ir(111) substrate is modeled with a slab of three atomic layers using a lattice constant of 3.847 Å, which we obtained from relaxed bulk Ir calculations, in agreement with Refs. [39,40]. We relax the top two layers, which reduces their separation by  $\Delta d_{12} = -2.1\%$  and  $\Delta d_{23} = -2.0\%$ . The calculated top-layer contraction is in good agreement with Refs. [41,42], while the second-layer contraction  $\Delta d_{23}$  is slightly larger compared to reference studies with small supercells and thicker slabs. We separate the periodic Ir(111) slabs by ca. 50 Å of vacuum.

For Gr, we obtain a relaxed lattice constant of 2.465 Å in agreement with previous studies [43,44]. The commensurate size of a Gr/Ir(111) supercell would be  $10.32 \times 10.32$  Gr/ $9.32 \times 9.32$  Ir, acquired from the experimental Moiré pattern [45]. In this study, we employ  $10 \times 10$  Gr/ $9 \times 9$  Ir and  $11 \times 11$  Gr/ $10 \times 10$  Ir supercell models with different

coverages of intercalated O. In these models, the periodic images of adsorbed F<sub>4</sub>TCNQ and TTF molecules are separated laterally by over 15 Å and thus have negligible mutual interaction. We fix the Ir lattice constant to its bulk value and adjust the Gr lattice to the Ir supercell. This results in minimal strain (+0.7 and  $-0.3\%$ ) for  $10 \times 10$  and  $11 \times 11$  Gr, respectively, with compression (stretching) denoted by positive (negative) signs. These supercell models provide periodic systems with nominal strain and allow studying varying coverages of intercalated O without edge defects.

The intercalating O atoms are placed at the hollow FCC sites of the Ir(111) surface, which are the most stable adsorption sites of atomic O [46]. With 0.11, 0.33, and 0.67 O monolayers (ML) coverages, we obtain defect-free periodic structures using the  $9 \times 9$  Ir(111) supercell (cell dimensions  $a = b = 24.48$ ,  $c = 63.33$  Å) as shown in Fig. 1. With the  $10 \times 10$  Ir(111) supercell ( $a = b = 27.20$ ,  $c = 63.33$  Å), we can model 0.5 ML O coverage, which is the saturated coverage in experiments [10,47].

### B. Adsorbate structure identification

We use the recently developed BOSS method [22,23,25–27] to identify the stable adsorbate structures of F<sub>4</sub>TCNQ and TTF on Gr (Fig. 2). We combine BOSS with DFT for accurate sampling of adsorption energies, with the same computational approach as before. To reduce the degrees of freedom and explore molecular packing, we treat the stable aromatic molecules as rigid *building blocks* (BBs) [49]. These molecules are strongly conjugated and known to maintain their shape upon adsorption, so they are well approximated with rigid BBs. The AES is then expressed in a configurational space of BB translations and rotations. Flat aromatic molecules typically adsorb flat on Gr via dispersive bonding. We therefore exclude the degrees of freedom related to molecular tilting and adsorption height.

We construct the AES in three dimensions (3D) as a function of the diffusion of the molecule on the surface ( $x$ - $y$ ) and its in-plane rotation ( $\gamma$  axis perpendicular to the surface). With reduced search dimensions, we can converge the model with fewer energy calculations without compromising its accuracy. The search is carried out within the Gr unit cell ( $x, y \in [0, 1]$ ) (fractional unit-cell coordinates) and in-plane orientation angles  $\gamma \in [0, 180]^\circ$ , which corresponds to a full period due to molecule symmetry. The adsorption energy is calculated as  $E_{\text{ads}} = E_{\text{tot}} - (E_{\text{Gr}} + E_{\text{mol}})$ , in which  $E_{\text{tot}}$  is the total energy of Gr with the adsorbed molecule,  $E_{\text{Gr}}$  is the energy of clean isolated Gr, and  $E_{\text{mol}}$  is the energy of an isolated F<sub>4</sub>TCNQ or TTF molecule.

Model refinement is carried out until the lowest energy minima have converged [23,26]. We inspect stable structures only in a range of  $\approx 25$  meV, which corresponds to the thermal energy at room temperature ( $E_T$ ), and will include the most probable candidate structures for monolayer self-assembly. We consider the adsorbates in their *ranking* order in terms of the adsorption energy relative to the global minimum ( $\Delta E_R$ ). The identified stable structures are refined with full relaxation in DFT using *tight* settings, in which we remove the BB approximation and allow motion of all atoms according to their interatomic forces. We verify the accuracy of our approximate

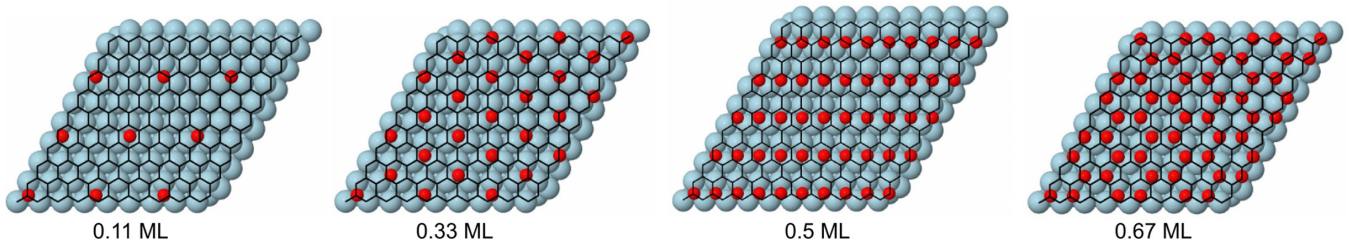


FIG. 1. Gr/O/Ir(111) supercell models with O coverages from 0.11 to 0.67 monolayers (ML).

model of supported Gr by relaxing the structures on the full Gr/O/Ir(111) substrate using *light* settings.

### III. RESULTS

#### A. Modeling electronically decoupled Gr

For the structure search of adsorbate configurations of  $F_4TCNQ$  and TTF on Gr/O/Ir(111), we first build a model of the entire substrate. We then explore ways to omit the supporting O/Ir structure while retaining an accurate description of adsorption on Gr.

##### 1. Electronic decoupling of Gr from Ir(111) via O intercalation

Gr binds to Ir(111) mainly via physisorption, but previous studies have also demonstrated local covalent bonding [47,48]. The hybridization of the electronic states and the corrugation of Gr due to the Gr/Ir(111) lattice mismatch deform the Dirac cone in the pDOS of Gr [Fig. 3(a)]. In electronically decoupled Gr, we expect to see its electronic and structural properties restored, that is, an undeformed Dirac cone and reduced structural corrugation.

Introducing O atoms in between Ir and Gr (known as intercalation) both passivates the Ir surface and physically displaces the Gr layer away from the metal substrate. This results in electronic decoupling of Gr, which we observe in the pDOS of Gr [Fig. 3(a)], with an undeformed Dirac cone at O coverages of 0.33 ML and above. This indicates that Gr is electronically decoupled already at low O coverages. Intercalation induces *p*-doping in Gr, which shifts the Dirac cone towards positive energies, in the range [+0.6, +0.7] eV with coverages [0.33, 1] ML (Table I).

We observe a decrease in Gr corrugation with increasing O coverage [Fig. 3(b) and Table I]. The corrugation is minimal

( $\Delta d_{Gr} < 0.1$  Å) for O coverages of 0.33 ML and higher, which indicates electronic decoupling already at low O coverages, in agreement with our pDOS observations. Intercalation increases the separation between Gr and the Ir surface in the range [3.47, 4.26] Å with O coverages [0, 1] ML. These findings are in agreement with previous studies [8,9,47,48].

We also investigated how O intercalation affects the charge of Gr by analyzing the Mulliken partial charges [50]. In nonintercalated Gr/Ir(111), Gr is *p*-doped by +0.004  $e$  (elementary charge,  $e = |e^-|$ ) per C atom (Table I). Intercalated O atoms draw electrons from the Ir surface and the Gr layer, increasing the doping of Gr to +0.012  $e$  with 1 ML O coverage. For the experimental saturated coverage of 0.5 ML [10,47], the Gr charge amounts to +0.008  $e$  per C atom, which we employ in the following section with manually charged freestanding Gr.

##### 2. Approximate model of intercalated Gr

When approximating the substrate, it is important that the description of molecular adsorption on it is well preserved. We analyze the adsorption properties of  $F_4TCNQ$  and TTF on Gr/O/Ir(111) (0.5 ML O coverage) using the most stable adsorbate structures (Fig. 2) identified in previous studies [28–30,51–53], and we relax the structures (Sec. III B) with *tight* calculation settings. We establish an approximate model of the substrate by studying the adsorption with different models of freestanding Gr and compare them against Gr/O/Ir(111). Via this comparison, we identify the closest approximation to the Gr/O/Ir(111) substrate.

We first analyze the molecules on Gr/O/Ir(111) in terms of their adsorption energy and geometry, the pDOS, and the charge distribution using the Mulliken analysis of partial charges. For the global minimum configurations of  $F_4TCNQ$  and TTF, we obtain adsorption energies of  $-1.878$  and  $-1.528$  eV, respectively (Table II). Both molecules adsorb at

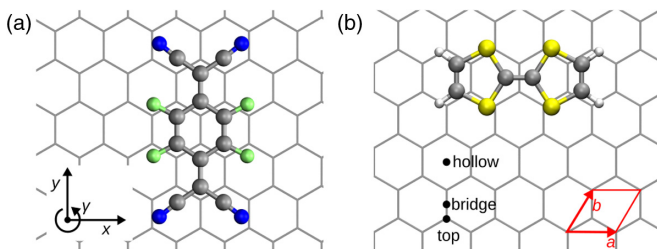


FIG. 2. Most stable structures of (a)  $F_4TCNQ$  and (b) TTF on Gr [28–30]. Search for all stable configurations is performed within the Gr unit cell (red) with respect to the translation of the molecule on the surface ( $x$ - $y$ ) and its in-plane rotation ( $\gamma$ ). The high-symmetry adsorption sites on Gr are hollow (*h*), bridge (*b*), and top (*t*).

TABLE I. Gr/O/Ir(111) structures with different O coverages ( $\theta_O$ ), showing the shift of the Dirac cone ( $\sigma$ ) in the pDOS of Gr, the height of Gr from the Ir surface ( $d_{Gr-Ir}$ ), the corrugation of Gr ( $\Delta d_{Gr}$ ), and the average charge per C atom in Gr ( $q_C$ ).

$\theta_O$ (ML)	$\sigma$ (eV)	$d_{Gr-Ir}$ (Å)	$\Delta d_{Gr}$ (Å)	$q_C$ ( $e$ )
0	0	3.47	0.33	+0.004
0.11	ca. +0.5	3.69	0.26	+0.004
0.33	+0.62	4.01	0.05	+0.007
0.5	+0.60	4.08	0.03	+0.008
0.67	+0.68	4.14	0.08	+0.010
1	+0.69	4.26	0.09	+0.012

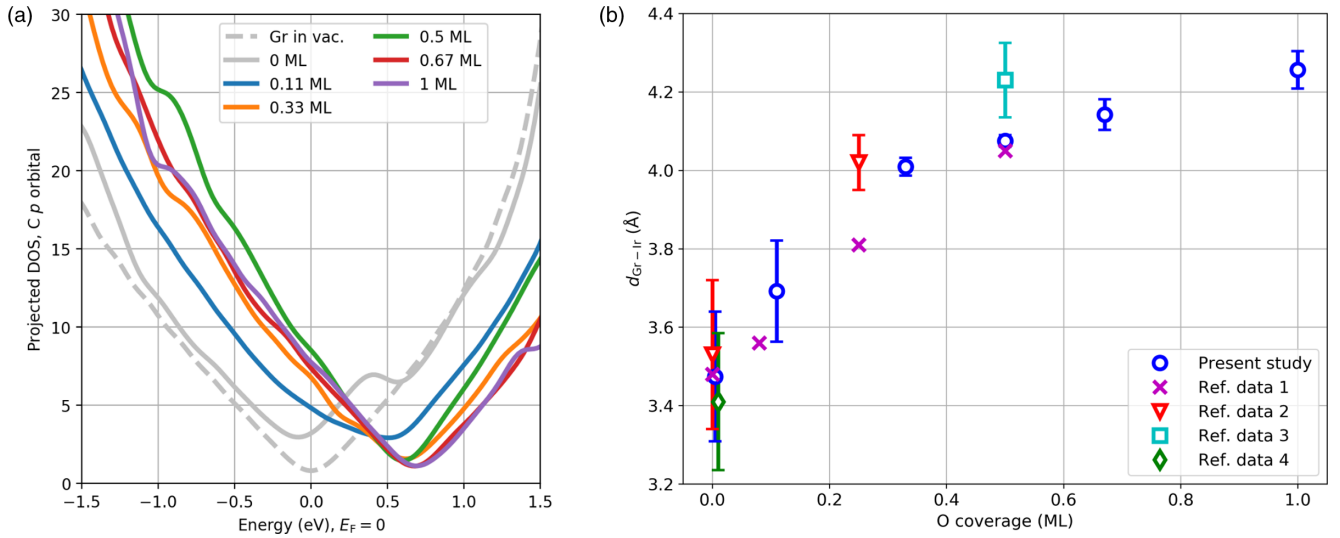


FIG. 3. (a) Projected DOS of C  $p$  orbitals in Gr with varying O coverages. (b) Height of Gr from the Ir surface ( $d_{\text{Gr-Ir}}$ ) as a function of O coverage. The error bars show the corrugation of Gr, i.e., the height of the lowest and highest atoms in the Gr layer. Reference data sets 1–4 originate from previous studies [8,9,47,48].

a similar height from Gr, ca. 3.3 Å. F<sub>4</sub>TCNQ adsorbs nearly flat ( $\Delta d_{\text{mol}} = 0.05$  Å) while TTF bends, such that its end H atoms are 0.26 Å closer to Gr compared to the center of the molecule. The adsorbed molecules cause indentation in Gr at the adsorption site, which increases layer corrugation from 0.03 Å (clean Gr) to ca. 0.1 Å.

The pDOSs of F<sub>4</sub>TCNQ [Fig. 4(b)] and TTF [Fig. 4(c)] show that, for both molecules, the electronic structure resembles that of an isolated molecule. Molecular pDOS contains narrow electronic states that indicate physisorption to Gr. In the partial charge distribution, we observe that F<sub>4</sub>TCNQ gains 0.3  $e$  and TTF donates 0.4  $e$ , as expected for electron acceptors and donors. The charge on Gr changes by the same amount (in comparison to clean Gr), which demonstrates that the transfer occurs mainly between Gr and the molecules. These findings suggest that the underlying O/Ir(111) structure has minimal effect on the adsorption properties of Gr. We therefore proceed to approximate the substrate using only freestanding Gr with

a manually set partial charge that corresponds to the positive doping of Gr in Gr/O/Ir(111) (+1.9  $e$  charge per  $11 \times 11$  Gr).

We employ two different approaches, in which we approximate  $p$ -doped Gr by (i) setting the total charge of the system (model  $Q$ ), and (ii) modifying the electronic structure of C species in Gr with fractionally occupied valence states ( $2p^{1.992}$ , model  $q_C$ ) [54–56]. For fractional occupation, we constrain the charge (+0.008  $e$  per C atom) to the Gr layer, while model  $Q$  introduces charge to the whole system, including the adsorbed molecule. We model the Gr layer as perfectly flat, which provides a good approximation of the minimally corrugated electronically decoupled Gr [Table I and Fig. 3(b)] and allows us to perform an adsorbate structure search within the periodic Gr unit cell [Fig. 2(b)]. The accuracy of the models is evaluated by comparing the adsorption properties of F<sub>4</sub>TCNQ and TTF on the two charged models ( $Q$  and  $q_C$ ) and on neutral freestanding Gr ( $Q_0$ ) against the Gr/O/Ir(111) substrate.

TABLE II. Adsorption properties of F<sub>4</sub>TCNQ and TTF on Gr/O/Ir(111) and on three different models of freestanding Gr: neutral ( $Q_0$ ), charged system ( $Q$ ), and modified C species of Gr ( $q_C$ ). The table shows the adsorption energy ( $E_{\text{ads}}$ ), the adsorption height of the molecule ( $d_{\text{mol-Gr}}$ ), the bending of the molecule ( $\Delta d_{\text{mol}}$ ), the corrugation of Gr ( $\Delta d_{\text{Gr}}$ ), the molecule charge ( $q_{\text{mol}}$ ), and the Gr charge ( $q_{\text{Gr}}$ ). Difference from Gr/O/Ir(111) is shown in parentheses (%).

F <sub>4</sub> TCNQ	$E_{\text{ads}}$ (eV)	$d_{\text{mol-Gr}}$ (Å)	$\Delta d_{\text{mol}}$ (Å)	$\Delta d_{\text{Gr}}$ (Å)	$q_{\text{mol}}$ ( $e$ )	$q_{\text{Gr}}$ ( $e$ )
Gr/O/Ir(111)	-1.878	3.25	0.05	0.11	-0.3	+2.1
$Q_0$	-1.795 (+4)	3.20 (-2)	0.06 (+22)	0.20 (+83)	-0.4 (-33)	+0.4 (-81)
$Q$	-1.619 (+14)	3.19 (-2)	0.09 (+93)	0.19 (+79)	-0.1 (+59)	+2.0 (-4)
$q_C$	-1.780 (+5)	3.19 (-2)	0.05 (+12)	0.20 (+83)	-0.3 (-19)	+2.2 (+7)
<b>TTF</b>						
Gr/O/Ir(111)	-1.528	3.31	0.26	0.12	+0.4	+1.5
$Q_0$	-1.174 (+23)	3.27 (-1)	0.30 (+12)	0.15 (+29)	+0.1 (-69)	-0.1 (-109)
$Q$	-1.598 (-5)	3.33 (+1)	0.12 (-55)	0.16 (+35)	+0.6 (+42)	+1.2 (-16)
$q_C$	-1.335 (+13)	3.26 (-2)	0.23 (-15)	0.20 (+69)	+0.4 (-8)	+1.5 (-1)



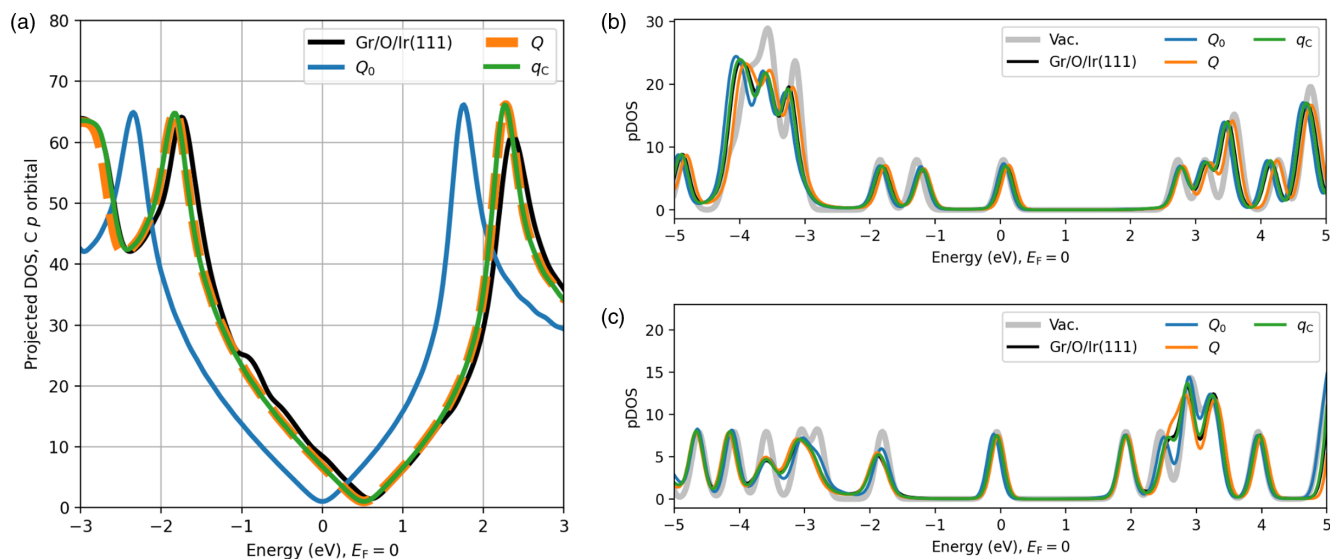


FIG. 4. (a) Projected DOS (pDOS) of C  $p$  orbitals in clean Gr (without adsorbed molecules), comparing the Gr/O/Ir(111) substrate (0.5 ML O coverage) to freestanding charge-neutral Gr ( $Q_0$ ), Gr with manually set total system charge ( $Q$ ), and charged C species ( $q_C$ ). (b) pDOS of  $F_4TCNQ$  in different charged systems, and (c) pDOS of TTF. For direct comparison, the pDOS of molecules in vacuum has been shifted by  $-0.6$  and  $+1.0$  eV for  $F_4TCNQ$  and TTF, respectively.

The adsorption energy of  $F_4TCNQ$  decreases in all freestanding Gr models, at most by 14% with the  $Q$  model (Table II). Conversely, for TTF, the  $Q$  model produces the best agreement, with 5% increase in the adsorption energy. In general, the differences in the energies are small and, considering both molecules, the best overall agreement is obtained with model  $q_C$ .

In the pDOS of clean Gr [Fig. 4(a)], we see that the Dirac cone is reproduced well with all approximate models. Its shift in the charged models ( $Q$  and  $q_C$ ) is ca.  $+0.5$  eV, in close agreement with Gr/O/Ir(111) ( $+0.6$  eV). The pDOS of  $F_4TCNQ$  [Fig. 4(b)] and TTF [Fig. 4(c)] features narrow electronic states, similar to Gr/O/Ir(111) with all approximate models. In particular, the highest occupied and lowest unoccupied molecular orbitals (HOMO and LUMO, respectively) near the Fermi level are identical in all models and independent of the charging method.

The partial charges of the molecules show that, without introducing any positive charge in the system (model  $Q_0$ ), the charges are overly negative ( $F_4TCNQ$ ) or not positive enough (TTF). Conversely, for charged systems (model  $Q$ ),  $F_4TCNQ$  is not negative enough and TTF is overly positive. The best approximation for molecular partial charges is clearly obtained with model  $q_C$ , in which the charges differ from Gr/O/Ir(111) by less than  $0.1 e$ . The charge of Gr is well approximated with both charged models ( $Q$  and  $q_C$ ), within 16%.

Overall, the differences between approximate models are small for the adsorption energies and heights of the molecules. The corrugation of Gr increases in all models with unsupported Gr as expected. By setting the total charge of the system (model  $Q$ ), the adsorption geometry of the molecules (flat  $F_4TCNQ$ , bent TTF) and their partial charges are poorly approximated. Also neutral Gr (model  $Q_0$ ) fails to reproduce the correct charges, for both the molecules and the Gr. Considering all analyzed properties for both molecules, we

conclude that the closest approximation to Gr/O/Ir(111) is obtained with model  $q_C$ . Hereafter, we refer to this model as “supported Gr” and employ it in the following Sec. III B to identify the stable structures of  $F_4TCNQ$  and TTF on Gr/O/Ir(111).

## B. Candidate structures of $F_4TCNQ$ and TTF for monolayer assembly

### 1. $F_4TCNQ$ and TTF on supported Gr model

We identify the stable structures of  $F_4TCNQ$  and TTF on a supported Gr model using the BOSS method. The Gr layer and the adsorbed molecule structures are considered to be BBs. The Gr layer features an  $11 \times 11$  unit cell (242 C atoms), charged via fractional occupation of C valence states (model  $q_C$  in the previous section). For the molecular BBs, we normalize the bond lengths and angles to their average values, so that we can utilize molecular symmetry for the in-plane rotation ( $\gamma$ ) (Fig. 2). TTF bends when adsorbed on Gr ( $\Delta d_{\text{mol}} = 0.23$  Å), such that the H atoms at both ends of the molecule are ca.  $0.2$  Å closer to the surface compared to the center of the molecule (Table II). This minimum configuration is adopted as a BB in our structure search. Bending of  $F_4TCNQ$  on Gr is below  $0.1$  Å and we employ a flat molecule as a BB.

We build the surrogate AES models for both molecules in 3D as a function of their translation on the surface ( $x$ - $y$ , within the Gr unit cell) and in-plane rotation ( $\gamma$ , full period) (Fig. 2). The height of the molecules from Gr is fixed to  $d_{F_4-Gr} = 3.3$  Å and  $d_{TTF-Gr} = 3.4$  Å. The adsorption energies are sampled with DFT and the surrogate models are converged with 500 energy acquisitions each. The calculation data are available in the NOMAD [57] and Zenodo [58] repositories.

We denote the stable structures according to their adsorption site and orientation on Gr (Fig. 2). The first letter is the high-symmetry adsorption site [hollow (*h*), bridge (*b*), or top (*t*)], given with respect to the center of the molecule. Configurations where one of the C atoms of the molecule is located at the top site of Gr (i.e., C atoms aligned) are denoted with the first letter being *C*. The second letter is the orientation of the molecule (*x*, *y*) with respect to its long symmetry axis.

We extract the stable configurations of F<sub>4</sub>TCNQ and TTF from the AES minima and refine them with full relaxation by removing the BB approximation. We identify two low-energy adsorbates for F<sub>4</sub>TCNQ. The global minimum structure is *by* with  $E_{\text{ads}} = -1.732$  eV. We find another structure *hx* with  $\Delta E_{\text{R}} = +35$  meV above the global minimum ( $E_{\text{ads}} = -1.696$  eV). This is already above  $E_{\text{T}}$ , so we do not analyze higher-energy structures. vdW interactions contribute 90% to the adsorption energy, indicating dispersive bonding. The adsorption height of F<sub>4</sub>TCNQ is 3.22 Å in both configurations and the adsorbed molecules are nearly flat ( $\Delta d_{\text{mol}} < 0.05$  Å). Charge transfer from Gr to F<sub>4</sub>TCNQ is 0.5 *e*, which is expected considering its high electron affinity (2.8 eV [59,60]). The pDOSs of the molecule exhibit narrow energy states, similar to isolated molecules, which indicates that F<sub>4</sub>TCNQ physisorbs to Gr in both identified structures.

For TTF, we detect two structures, *bx* and *Cy*, that compete for the global minimum with nearly equal energies (within 2 meV). The lowest energy is given by configuration *bx* with  $E_{\text{ads}} = -1.163$  eV and the structure *Cy* has  $E_{\text{ads}} = -1.161$  eV. Both configurations exhibit similar adsorption heights (3.25 and 3.33 Å for *bx* and *Cy*, respectively) and molecular bending (0.27 and 0.33 Å). These values correspond closely to the bending of the initial BB geometry (0.2 Å) and thus justify the approximation. Similar to F<sub>4</sub>TCNQ, both TTF structures are physisorbed to Gr. We observe a charge transfer of 0.3 *e* from TTF to Gr, as expected for an electron donor.

For both F<sub>4</sub>TCNQ and TTF, we also identify variants of the high-symmetry configurations near the corresponding AES minima. These structures have almost equal energies (within 10 meV) compared to their high-symmetry counterparts and feature small rotations (less than 10°) and shifts from the high-symmetry adsorption sites. These are likely artifacts that originate from energy fluctuations in the broad AES minima and we do not report them as separate configurations.

## 2. Comparison of adsorbate solutions across studies

Lastly, we compare our findings to previous studies of F<sub>4</sub>TCNQ and TTF adsorption on Gr. In other works, the molecules were simulated on freestanding Gr only, in contrast to our study. Stable adsorbate structures were identified by relaxing the molecules above three high-symmetry adsorption sites [hollow (*h*), bridge (*b*), and top (*t*), Fig. 2] in two molecular orientations, *x* and *y*. All six configurations were found to be local minima for both F<sub>4</sub>TCNQ [28,29] and TTF [30], with global minimum structures *by* and *bx*, respectively. Previous studies have applied a level of theory (PBE + vdW) similar to ours so we expect the potential difference to be indicative of substrate effects and not DFT artifacts.

TABLE III. Stable structures of F<sub>4</sub>TCNQ and TTF on Gr, showing the adsorption energies of the molecular building blocks ( $E_{\text{B}}$ ), the relaxed structures ( $E_{\text{R}}$ ), and the energies of the relaxed structures relative to the global minimum ( $\Delta E_{\text{R}}$ ). Configurations included in the AES model are highlighted in boldface.

F <sub>4</sub> TCNQ	$E_{\text{B}}$ (eV)	$E_{\text{R}}$ (eV)	$\Delta E_{\text{R}}$ (eV)
<i>by</i>	-1.706	-1.732	0
<b><i>hx</i></b>	-1.662	-1.696	+0.035
<i>tx</i>	-1.606	-1.659	+0.072
<i>hy</i>	-1.587	-1.636	+0.095
TTF			
<b><i>bx</i></b>	-1.122	-1.163	0
<b><i>Cy</i></b>	-1.123	-1.161	+0.002
<i>hy</i>	-1.114	-1.149	+0.014
<i>hx</i>	-1.104	-1.144	+0.018

In the previous section, we detected two low-energy structures for both molecules. To verify that we have not overlooked any low-energy configurations, we consider structures from previous studies and relax them on the supported Gr model. For F<sub>4</sub>TCNQ, we find that our identified structures *by* and *hx* are still the lowest in energy. The next structures in energy ranking are *tx* and *hy*, which are clearly above the global minimum by  $\Delta E_{\text{R}} + 72$  and  $+95$  meV, respectively [Figs. 5(a) and 6(a), and Table III]. These structures are well above  $E_{\text{T}}$  (25 meV), so we do not consider them further.

We discover that our TTF structures *bx* and the previously unreported structure *Cy* have the lowest energies out of all adsorbates. The next structures in ranking are *hy* and *hx* with  $\Delta E_{\text{R}} + 14$  and  $+18$  meV, respectively [Figs. 5(b) and 6(b), and Table III]. Compared to F<sub>4</sub>TCNQ, the range of TTF adsorbate energies is much smaller and all four structures are within  $E_{\text{T}}$ . After these, the next structure in ranking is *by* (not shown here) with  $\Delta E_{\text{R}} + 41$  meV, which is beyond our consideration for candidate structures for film formation. Both F<sub>4</sub>TCNQ and TTF physisorb to Gr in all studied configurations, shown by the narrow energy states in their pDOSs (Fig. 7).

To further investigate the ranking of structures and whether the new TTF configuration *Cy* originates from our different model (supported Gr) or different methodology (global AES exploration), we relax all our local minima structures on freestanding Gr. For F<sub>4</sub>TCNQ, adsorption energies and ranking of structures are similar on both substrates; the global minimum structure *by* ( $E_{\text{ads}} = -1.751$  eV on freestanding Gr) is the same as on the supported Gr model, in agreement with previous studies [28,29,52,53]. For TTF, we obtain the same global minimum structure *bx* ( $E_{\text{ads}} = -1.049$  eV) on both substrates, which corresponds to previous studies [30,51,53]. The structure *Cy* remains stable also on freestanding Gr, with energy nearly identical to the global minimum ( $\Delta E_{\text{R}} = +4$  meV).

We also verify the accuracy of the substrate approximation by relaxing the adsorbates on the full Gr/O/Ir(111) substrate. We observe only negligible differences in the relative adsorption energies (below 10 meV, Fig. 6). The ranking of the structures remains unchanged between the approximated and the full Gr/O/Ir(111) substrate (excluding a single change

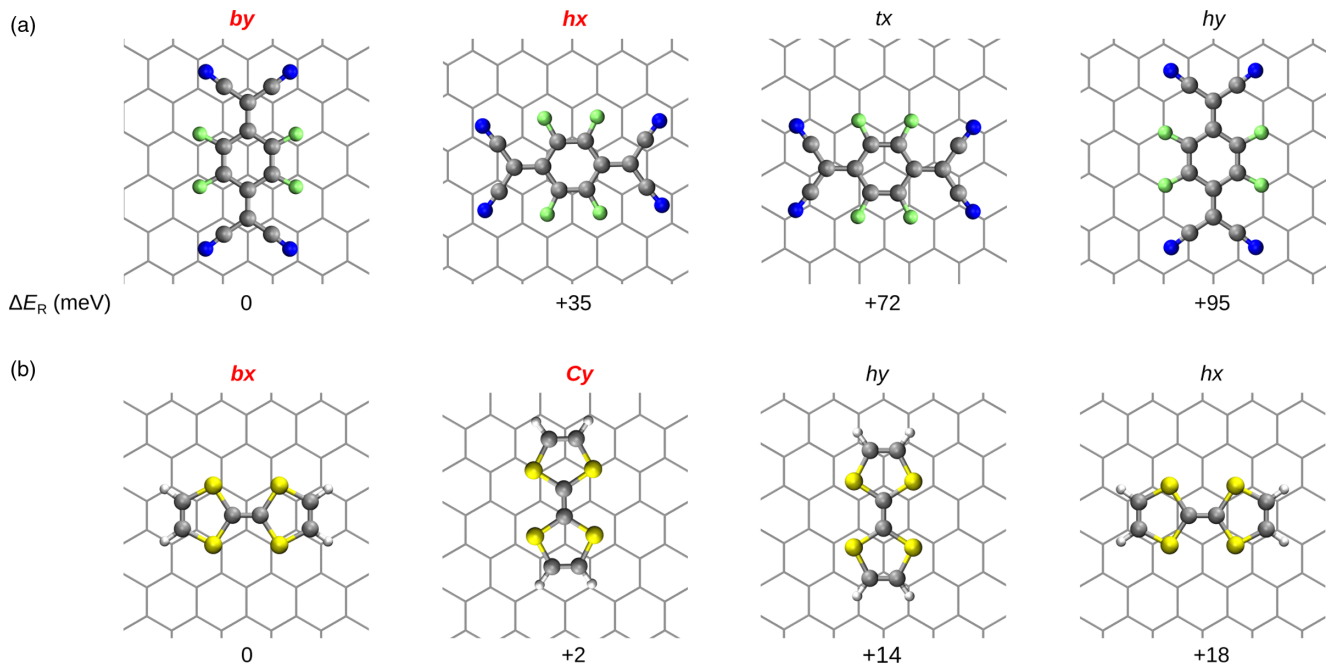


FIG. 5. Stable structures of (a) F<sub>4</sub>TCNQ and (b) TTF and their adsorption energies relative to the global minimum ( $\Delta E_R$ ). Configurations included in the AES model (low-energy structures) are highlighted in red.

between two TTF configurations with nearly identical energies). This shows that the approximate model is viable for describing the adsorption of F<sub>4</sub>TCNQ and TTF on supported Gr.

#### IV. DISCUSSION

By studying different coverages of intercalated O in Gr/O/Ir(111), we established that intercalation electronically decouples the states of graphene from the Ir(111) surface from

0.3 ML coverage onwards. We note that the corrugation of Gr with 0.5 ML O coverage is smaller than previously reported by Jolie *et al.* [47], which is likely due to nominal stretching of Gr (strain  $-0.3\%$ ) in the  $10 \times 10$  Ir supercell. We recommend this model size for further studies instead of  $9 \times 9$  Ir, where compressive strain increases Gr corrugation.

Our model of supported Gr provides a good description of molecular adsorption of F<sub>4</sub>TCNQ and TTF on Gr/O/Ir(111) with respect to the adsorption energies, geometries, partial

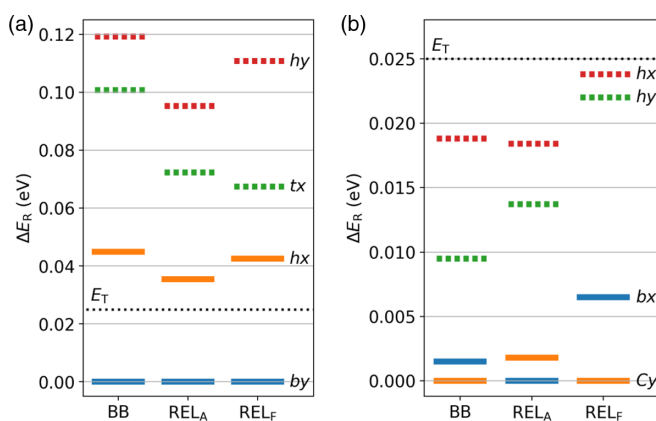


FIG. 6. Relative adsorption energy ( $\Delta E_R$ ) of (a) F<sub>4</sub>TCNQ and (b) TTF, given as the difference from the global energy minimum. Shown are the  $\Delta E_R$  of molecular building blocks (BB) and relaxed structures on the approximated substrate (REL<sub>A</sub>), and relaxed structures on the full Gr/O/Ir(111) substrate (REL<sub>F</sub>). Configurations included (excluded) in the AES model are shown with solid (dotted) lines. The energy ranges of different structures are 0.12 and 0.024 eV for F<sub>4</sub>TCNQ and TTF, respectively. Thermal energy at room temperature ( $E_T \approx 25$  meV) is indicated with a black dotted line.

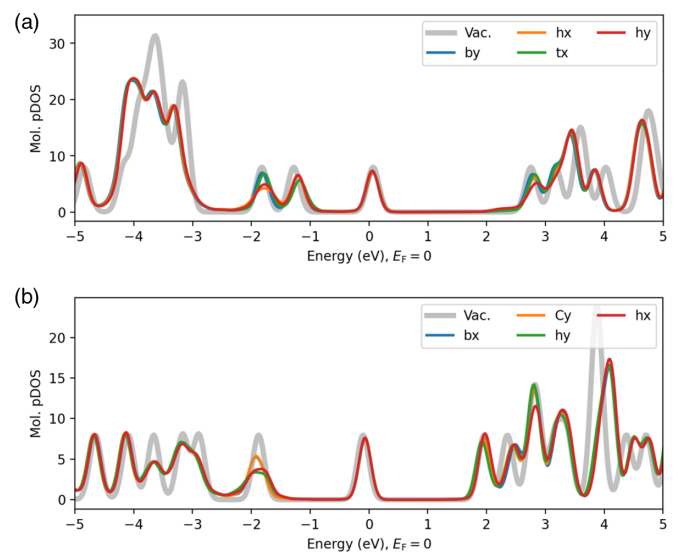


FIG. 7. PDOS of (a) F<sub>4</sub>TCNQ and (b) TTF molecules in the stable structures. For direct comparison, the pDOS of molecules in vacuum has been shifted by  $-0.7$  and  $+0.6$  eV for F<sub>4</sub>TCNQ and TTF, respectively.

charges, and pDOS. For charge-neutral Gr (model  $Q_0$ ), the partial charges of the molecules and the Gr layer are poorly approximated, which may affect molecular assembly in film formation. By omitting the Ir substrate and the intercalated O (in total 350 atoms) and applying their induced charge to Gr by altering the occupation of C  $2p$  states from 2 to 1.992 in the basis set representation, we reduced the energy computation time to 1% compared to the full substrate. This facilitates quick sampling of different molecular configurations and significantly speeds up AES exploration. Our approach can also be used for other materials to approximate computationally expensive substrates for molecular adsorption.

We found that  $F_4TCNQ$  and TTF physisorb on Gr in several different configurations. Refining the structures with full relaxation resulted in only minimal changes in their adsorption energy [on average  $-0.04$  eV (Fig. 6 and Table III)], which shows that the BB approximation is valid for these molecules. Overall, the relaxation did not affect the ranking of the structures, excluding the two TTF configurations that compete for the global minimum [Fig. 6(b)]. Further checks with the full Gr/O/Ir(111) substrate confirmed that the approximate substrate model correctly accounts for adsorption.

Considering candidate structures for film formation, two  $F_4TCNQ$  structures with the lowest energies (within 35 meV) may be employed as building blocks to study monolayer self-assembly. For TTF, the structures are nearly indistinguishable by energy, implying that the molecule diffuses freely at room temperature. Therefore, we have no well-defined TTF adsorbates (neither by binding site nor orientation). In monolayer formation, it may be expected that  $F_4TCNQ$  binds to the surface while TTF is arranged around other molecules according to electrostatic interactions. This suggests that the structure and the stability of  $F_4TCNQ$ /TTF CTCs are mostly governed by molecule-molecule interactions.

Our identified minimum-energy structures of  $F_4TCNQ$  and TTF are in agreement with literature reports. The previously unreported TTF structure  $Cy$  is stable on both supported and freestanding Gr, so its discovery can be attributed to thorough investigation of low-energy adsorbates with the BOSS method. This highlights the importance of smart sampling in structure search and how less obvious structures can be missed with the traditional approach of investigating only high-symmetry configurations.

The number of energy calculations required to infer local minima with BOSS is small compared to other methods of AES exploration, such as grid search. In this study, the number of calculations needed to construct the 3D AES (500 points per molecule) is only 6% of computing a grid with sufficient point density to reliably detect all local minima (ca. 20 points per dimension).

## V. CONCLUSION

In this study, we present an approximate model of the Gr/O/Ir(111) substrate using unsupported Gr with manually doped C species. We applied the model to identify the stable adsorbate structures of  $F_4TCNQ$  and TTF on supported Gr using the BOSS active learning approach. The detected adsorbate structures at the approximate substrate match those on the full substrate, but at only 1% of the total computational cost. The presented method can also be applied with other intercalated substrates and organic adsorbates.

Both molecules physisorb to Gr, but we expect only  $F_4TCNQ$  to have discrete adsorption configurations. In monolayer assembly, TTF may arrange freely via intermolecular interactions and we estimate electronically decoupled Gr to have little effect on film morphologies.

The established model of supported Gr is computationally affordable and facilitates *ab initio* energy sampling with large supercell models. Combined with BOSS, the model enables global structure search of CTC configurations using multiple molecules. The acquired knowledge can help in verifying the precise structural phases of CTCs observed in experiments [15].

## ACKNOWLEDGMENTS

The authors wish to acknowledge Dr. V. Havu for insightful discussions. M.T. and P.R. have received funding from the Academy of Finland via the Artificial Intelligence for Microscopic Structure Search (AIMSS) Project No. 316601 and the Flagship Programme: Finnish Center for Artificial Intelligence FCAI. J.J. has been funded by the Emil Aaltonen Foundation. Generous computational resources were provided by CSC – IT Center for Science, Finland, and the Aalto Science-IT project.

- 
- [1] Y. Muraoka, S. Yamashita, T. Yamamoto, and Y. Nakazawa, Microchip-calorimetry of organic charge transfer complex which shows superconductivity at low temperatures, *Thermochim. Acta* **532**, 88 (2012).
  - [2] M. Dressel, Ordering phenomena in quasi-one-dimensional organic conductors, *Naturwissenschaften* **94**, 527 (2007).
  - [3] N. Gonzalez-Lakunza, I. Fernández-Torrente, K. J. Franke, N. Lorente, A. Arnau, and J. I. Pascual, Formation of Dispersive Hybrid Bands at an Organic-Metal Interface, *Phys. Rev. Lett.* **100**, 156805 (2008).
  - [4] S. Jeon, P. W. Doak, B. G. Sumpter, P. Ganesh, and P. Maksymovych, Thermodynamic control of two-dimensional molecular ionic nanostructures on metal surfaces, *ACS Nano* **10**, 7821 (2016).
  - [5] S. Maier and M. Stöhr, Molecular assemblies on surfaces: Towards physical and electronic decoupling of organic molecules, *Beilstein J. Nanotechnol.* **12**, 950 (2021).
  - [6] E. Starodub, N. C. Bartelt, and K. F. McCarty, Oxidation of graphene on metals, *J. Phys. Chem. C* **114**, 5134 (2010).
  - [7] R. Larciprete, S. Ulstrup, P. Lacovig, M. Dalmiglio, M. Bianchi, F. Mazzola, L. Hornekær, F. Orlando, A. Baraldi, P. Hofmann, and S. Lizzit, Oxygen switching of the epitaxial graphene-metal interaction, *ACS Nano* **6**, 9551 (2012).
  - [8] S. Ulstrup, M. Andersen, M. Bianchi, L. Barreto, B. Hammer, L. Hornekær, and P. Hofmann, Sequential oxygen and alkali intercalation of epitaxial graphene on Ir(111): Enhanced many-body effects and formation of *pn*-interfaces, *2D Mater.* **1**, 025002 (2014).



- [9] M. Andersen, L. Hornekær, and B. Hammer, Understanding intercalation structures formed under graphene on Ir(111), *Phys. Rev. B* **90**, 155428 (2014).
- [10] A. J. Martínez-Galera, U. A. Schröder, F. Huttman, W. Jolie, F. Craes, C. Busse, V. Caciuc, N. Atodiresi, S. Blügel, and T. Michely, Oxygen orders differently under graphene: New superstructures on Ir(111), *Nanoscale* **8**, 1932 (2016).
- [11] U. A. Schröder, M. Petrović, T. Gerber, A. J. Martínez-Galera, E. Grånäs, M. A. Arman, C. Herbig, J. Schnadt, M. Kralj, J. Knudsen, and T. Michely, Core level shifts of intercalated graphene, *2D Mater.* **4**, 015013 (2017).
- [12] J. T. Sun, Y. H. Lu, W. Chen, Y. P. Feng, and A. T. S. Wee, Linear tuning of charge carriers in graphene by organic molecules and charge-transfer complexes, *Phys. Rev. B* **81**, 155403 (2010).
- [13] Y. Yang, G. Liu, J. Liu, M. Wei, Z. Wang, X. Hao, D. V. Maheswar Repaka, R. V. Ramanujan, X. Tao, W. Qin, and Q. Zhang, Anisotropic magnetoelectric coupling and Cotton–Mouton effects in the organic magnetic charge-transfer complex pyrene-F<sub>4</sub>TCNQ, *ACS Appl. Mater. Interfaces* **10**, 44654 (2018).
- [14] L. Wu, F. Wu, Q. Sun, J. Shi, A. Xie, X. Zhu, and W. Dong, A TTF–TCNQ complex: An organic charge-transfer system with extraordinary electromagnetic response behavior, *J. Mater. Chem. C* **9**, 3316 (2021).
- [15] A. Kumar, K. Banerjee, M. M. Ervasti, S. Kezilebieke, M. Dvorak, P. Rinke, A. Harju, and P. Liljeroth, Electronic characterization of a charge-transfer complex monolayer on graphene, *ACS Nano* **15**, 9945 (2021).
- [16] P. Hohenberg and W. Kohn, Inhomogeneous electron gas, *Phys. Rev.* **136**, B864 (1964).
- [17] W. Kohn and L. J. Sham, Self-consistent equations including exchange and correlation effects, *Phys. Rev.* **140**, A1133 (1965).
- [18] B. Shahriari, K. Swersky, Z. Wang, R. P. Adams, and N. de Freitas, Taking the human out of the loop: A review of Bayesian optimization, *Proc. IEEE* **104**, 148 (2016).
- [19] S. Carr, R. Garnett, and C. Lo, BASC: Applying Bayesian optimization to the search for global minima on potential energy surfaces, in *Proceedings of the 33rd International Conference on Machine Learning*, edited by M. F. Balcan and K. Q. Weinberger, Vol. 48 (PMLR, New York, 2016), pp. 898–907.
- [20] M. S. Jørgensen, U. F. Larsen, K. W. Jacobsen, and B. Hammer, Exploration versus exploitation in global atomistic structure optimization, *J. Phys. Chem. A* **122**, 1504 (2018).
- [21] E. Garijo del Río, J. J. Mortensen, and K. W. Jacobsen, Local Bayesian optimizer for atomic structures, *Phys. Rev. B* **100**, 104103 (2019).
- [22] M. Todorović, M. U. Gutmann, J. Corander, and P. Rinke, Bayesian inference of atomistic structure in functional materials, *npj Comput. Mater.* **5**, 35 (2019).
- [23] J. Järvi, P. Rinke, and M. Todorović, Detecting stable adsorbates of (1S)-camphor on Cu(111) with Bayesian optimization, *Beilstein J. Nanotechnol.* **11**, 1577 (2020).
- [24] D. M. Packwood and T. Hitosugi, Rapid prediction of molecule arrangements on metal surfaces via Bayesian optimization, *Appl. Phys. Express* **10**, 065502 (2017).
- [25] A. T. Egger, L. Hörmann, A. Jeindl, M. Scherbela, V. Obersteiner, M. Todorović, P. Rinke, and O. T. Hofmann, Charge transfer into organic thin films: A deeper insight through machine-learning-assisted structure search, *Adv. Sci.* **7**, 2000992 (2020).
- [26] L. Fang, E. Makkonen, M. Todorović, P. Rinke, and X. Chen, Efficient amino acid conformer search with Bayesian optimization, *J. Chem. Theory Comput.* **17**, 1955 (2021).
- [27] BOSS Code Repository, <https://gitlab.com/cest-group/boss> (accessed: April 2022).
- [28] I. S. S. de Oliveira and R. H. Miwa, Organic molecules deposited on graphene: A computational investigation of self-assembly and electronic structure, *J. Chem. Phys.* **142**, 044301 (2015).
- [29] S. Yang, Y. Jiang, S. Li, and W. Liu, Many-body dispersion effects on the binding of TCNQ and F4-TCNQ with graphene, *Carbon* **111**, 513 (2017).
- [30] J. B. de Oliveira, I. S. S. de Oliveira, J. E. Padilha, and R. H. Miwa, Tunable magnetism and spin-polarized electronic transport in graphene mediated by molecular functionalization of extended defects, *Phys. Rev. B* **97**, 045107 (2018).
- [31] V. Blum, R. Gehrke, F. Hanke, P. Havu, V. Havu, X. Ren, K. Reuter, and M. Scheffler, Ab initio molecular simulations with numeric atom-centered orbitals, *Comput. Phys. Commun.* **180**, 2175 (2009).
- [32] V. Havu, V. Blum, P. Havu, and M. Scheffler, Efficient  $O(N)$  integration for all-electron electronic structure calculation using numeric basis functions, *J. Comput. Phys.* **228**, 8367 (2009).
- [33] X. Ren, P. Rinke, V. Blum, J. Wieferink, A. Tkatchenko, A. Sanfilippo, K. Reuter, and M. Scheffler, Resolution-of-identity approach to Hartree–Fock, hybrid density functionals, RPA, MP2 and GW with numeric atom-centered orbital basis functions, *New J. Phys.* **14**, 053020 (2012).
- [34] J. P. Perdew, K. Burke, and M. Ernzerhof, Generalized Gradient Approximation Made Simple, *Phys. Rev. Lett.* **77**, 3865 (1996).
- [35] A. Tkatchenko and M. Scheffler, Accurate Molecular Van Der Waals Interactions from Ground-State Electron Density and Free-Atom Reference Data, *Phys. Rev. Lett.* **102**, 073005 (2009).
- [36] E. van Lenthe, E. J. Baerends, and J. G. Snijders, Relativistic regular two-component Hamiltonians, *J. Chem. Phys.* **99**, 4597 (1993).
- [37] J. Neugebauer and M. Scheffler, Adsorbate-substrate and adsorbate-adsorbate interactions of Na and K adlayers on Al(111), *Phys. Rev. B* **46**, 16067 (1992).
- [38] J. L. C. Fajín, M. N. D. S. Cordeiro, J. R. B. Gomes, and F. Illas, On the need for spin polarization in heterogeneously catalyzed reactions on nonmagnetic metallic surfaces, *J. Chem. Theory Comput.* **8**, 1737 (2012).
- [39] S. D. Miller, N. İnoğlu, and J. R. Kitchin, Configurational correlations in the coverage dependent adsorption energies of oxygen atoms on late transition metal fcc(111) surfaces, *J. Chem. Phys.* **134**, 104709 (2011).
- [40] J. Carrasco, W. Liu, A. Michaelides, and A. Tkatchenko, Insight into the description of van der Waals forces for benzene adsorption on transition metal (111) surfaces, *J. Chem. Phys.* **140**, 084704 (2014).
- [41] V. Zólyomi, J. Kollár, and L. Vitos, On the surface relaxation of transition metals, *Philos. Mag.* **88**, 2709 (2008).
- [42] H. Zhang and W.-X. Li, First-principles investigation of surface and subsurface H adsorption on Ir(111), *J. Phys. Chem. C* **113**, 21361 (2009).

- [43] H.-J. Kim and J.-H. Cho, Fluorine-induced local magnetic moment in graphene: A hybrid DFT study, *Phys. Rev. B* **87**, 174435 (2013).
- [44] W. Zhang, X. Yu, E. Cahyadi, Y.-H. Xie, and C. Ratsch, On the kinetic barriers of graphene homo-epitaxy, *Appl. Phys. Lett.* **105**, 221607 (2014).
- [45] A. T. N'Diaye, J. Coraux, T. N. Plasa, C. Busse, and T. Michely, Structure of epitaxial graphene on Ir(111), *New J. Phys.* **10**, 043033 (2008).
- [46] W. P. Krekelberg, J. Greeley, and M. Mavrikakis, Atomic and molecular adsorption on Ir(111), *J. Phys. Chem. B* **108**, 987 (2004).
- [47] W. Jolie, F. Craes, M. Petrović, N. Atodiresei, V. Caciuc, S. Blügel, M. Kralj, T. Michely, and C. Busse, Confinement of Dirac electrons in graphene quantum dots, *Phys. Rev. B* **89**, 155435 (2014).
- [48] C. Busse, P. Lazić, R. Djemour, J. Coraux, T. Gerber, N. Atodiresei, V. Caciuc, R. Brako, A. T. N'Diaye, S. Blügel, J. Zegenhagen, and T. Michely, Graphene on Ir(111): Physisorption with Chemical Modulation, *Phys. Rev. Lett.* **107**, 036101 (2011).
- [49] A. R. Oganov and C. W. Glass, Crystal structure prediction using ab initio evolutionary techniques: Principles and applications, *J. Chem. Phys.* **124**, 244704 (2006).
- [50] R. S. Mulliken, Electronic population analysis on LCAO-MO molecular wave functions. I, *J. Chem. Phys.* **23**, 1833 (1955).
- [51] Y.-H. Zhang, K.-G. Zhou, K.-F. Xie, J. Zeng, H.-L. Zhang, and Y. Peng, Tuning the electronic structure and transport properties of graphene by noncovalent functionalization: Effects of organic donor, acceptor and metal atoms, *Nanotechnology* **21**, 065201 (2010).
- [52] M. Chi and Y.-P. Zhao, First principle study of the interaction and charge transfer between graphene and organic molecules, *Comput. Mater. Sci.* **56**, 79 (2012).
- [53] P. A. Denis, Chemical reactivity of electron-doped and hole-doped graphene, *J. Phys. Chem. C* **117**, 3895 (2013).
- [54] N. Moll, Y. Xu, O. T. Hofmann, and P. Rinke, Stabilization of semiconductor surfaces through bulk dopants, *New J. Phys.* **15**, 083009 (2013).
- [55] O. Sinai, O. T. Hofmann, P. Rinke, M. Scheffler, G. Heimel, and L. Kronik, Multiscale approach to the electronic structure of doped semiconductor surfaces, *Phys. Rev. B* **91**, 075311 (2015).
- [56] J. Stähler and P. Rinke, Global and local aspects of the surface potential landscape for energy level alignment at organic-ZnO interfaces, *Chem. Phys.* **485-486**, 149 (2017).
- [57] J. Järvi, M. Todorović, and P. Rinke, F<sub>4</sub>TCNQ and TTF adsorbed on Gr/O/Ir(111) and approximate supported Gr, NOMAD Repository (2022), doi:10.17172/NOMAD/2022.04.07-1.
- [58] J. Järvi, M. Todorović, and P. Rinke, F<sub>4</sub>TCNQ and TTF on approximate supported Gr, 3D surface adsorbate search with BOSS, Zenodo Repository (2022), doi:10.5281/zenodo.6421409.
- [59] D. A. Horke, G. M. Roberts, and J. R. R. Verlet, Excited states in electron-transfer reaction products: Ultrafast relaxation dynamics of an isolated acceptor radical anion, *J. Phys. Chem. A* **115**, 8369 (2011).
- [60] O. T. Hofmann, V. Atalla, N. Moll, P. Rinke, and M. Scheffler, Interface dipoles of organic molecules on Ag(111) in hybrid density-functional theory, *New J. Phys.* **15**, 123028 (2013).